Sterically-Controlled Excited-State Intramolecular Proton Transfer Dynamics in Solution

Jungkweon Choi,[a,b,†] Doo-Sik Ahn,[a,b,†] Sol-Yi Gal,[c] Dae Won Cho,[d] Cheolhee Yang,[a,b] Kyung-Ryang Wee,[c,] Hyotcherl Ihee[a,b,*]*

a. Center for Nanomaterials and Chemical Reactions, Institute for Basic Science, Daejeon 34141, Republic of Korea

b. Department of Chemistry and KI for the BioCentury, Korea Advanced Institute of Science and Technology (KAIST), Daejeon 305-701, Republic of Korea

c. Department of Chemistry and Institute of Natural Science, Daegu University, Gyeongsan 38453, Republic of Korea

d. Department of Advanced Materials Chemistry, Korea University, Sejong Campus, Sejong 30019, Korea

† These authors contributed equally.

* Corresponding author: Kyung-Ryang Wee and Hyotcherl Ihee

E-mail: krwee@daegu.ac.kr, hyotcherl.ihee@kaist.ac.kr

Experimental Section

Synthesis and Characterization: 1,10-phenanthroline-5,6-dione, salycilaldehyde, 5-fluoro-2-hydroxybenzenaldehyde, 2-hydroxy-5-methoxybenzaldehyde, 2-hydroxy-5-naphthaldehyde, aniline, and solvents were purchased from Sigma-Aldrich, JUNSEI, Duksan, TCI Co., and Chemical Oriental Chemical Industries and used without any purification. Deuterated solvent for NMR experiments was purchased from Merck. All reactions were monitored with thin layer chromatography (TLC) using a commercial TLC plate (Merck Co.). Silica gel column chromatography was performed on silica gel 60 G (230~400 mesh ASTM, Merck Co.). The synthesized compounds were characterized by ^{1}H-NMR and ^{13}C-NMR, mass spectrometry, and elemental analysis. The ^{1}H and proton-decoupled ^{13}C spectra were recorded on a Bruker500 spectrometer operating at (500 and 125) MHz, respectively, and all proton and carbon chemical shifts were measured relative to internal residual chloroform (99.5 % CDCl3) or dimethyl sulfoxide (99.5% DMSO-D$_6$) from the lock solvent. The elemental analyses (C, H, N, O) were performed using Thermo Fisher Scientific Flash 2000 series analyzer. High-resolution tandem mass (MRMS) spectrometry was performed using Jeol LTD JMS-HX 110/110A at the Korean Basic Science Institute. As shown in Scheme S1, four 2-(1-phenyl-1H-imidazo[4,5-f][1,10]phenanthrolin-2-yl) derivatives, PIPP-H, PIPP-F, PIPP-OMe, and PIPN, were successfully synthesized and the detail synthesis procedure are described below.
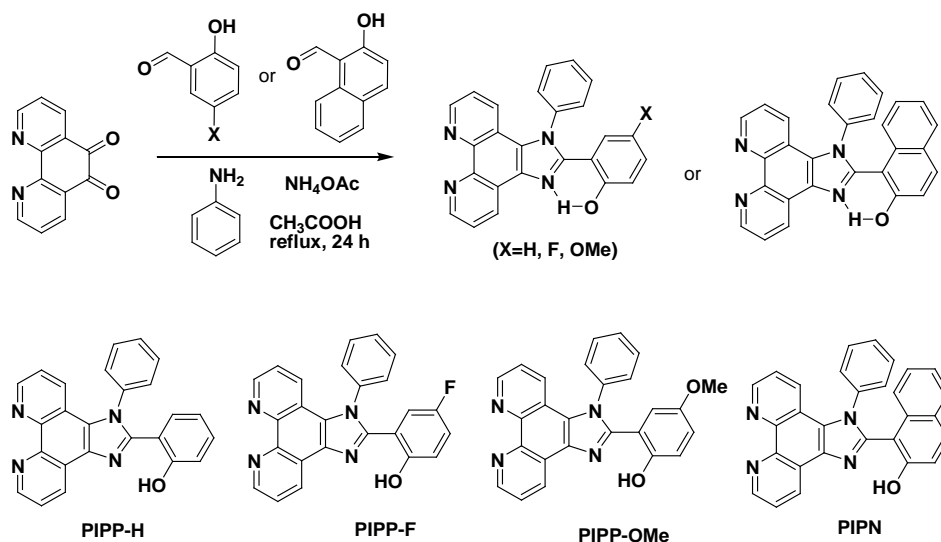
Scheme S1. Molecular structure and synthesis scheme for four ESIPT compounds (PIPP-H, PIPP-F, PIPP-OMe, and PIPN).

General synthesis of four ESIPT compounds (PIPP-H, PIPP-F, PIPP-OMe, and PIPN): Under an argon atmosphere, 0.9 mmol of aldehyde derivative (salycilaldehyde, 5-fluoro-2-hydroxybenzenaldehyde, 2-hydroxy-5-methoxybenzaldehyde, and 2-hydroxy-5-naphthaldehyde for PIPP-H, PIPP-F, PIPP-OMe, and PIPN, respectively) and aniline (83.8 mg, 0.9 mmol) were dissolved in glacial acetic acid (5 mL) and stirred for 20 min at room temperature. 1,10 phenanthroline-5,6-dione (189 mg, 0.9 mmol) and ammonium acetate (693 mg, 9 mmol, excess) were added. This mixture was refluxed at 125 °C overnight. The solution was cooled to room temperature and diluted with cool water (30 mL). The solid product was collected after filtration and washed with water. All of products were purified by silica-gel column chromatography using CH_2Cl_2:MeOH(15:1) eluent and further purified by recrystallization.

PIPP-H. Yield: 175mg, 50%. ^1H NMR (500 MHz, CDCl$_3$, ppm): δ 13.34 (s, 1 H), 9.25 (d, 1 H), 9.10 (t, 1 H), 9.04 (d, 1 H), 7.85-7.79 (m, 4 H), 7.68 (d, 2 H), 7.29 (d, 2H), 7.26 (t, 1 H), 7.16 (d, 1 H), 6.80 (d, 1 H), 6.56 (t, 1 H). ^{13}C NMR (125 MHz, CDCl$_3$, ppm): δ 206.9, 149.3, 148.3, 138.4, 131.4, 131.3, 131.1, 129.8, 128.8, 128.2, 126.2, 123.8, 122.4, 119.6, 118.4, 118.2, 112.6. HRMS Calcd for [$C_{25}H_{16}N_4O$]: 388.42 m/z, Found: 388.14 m/z. Anal. Found (Calc) for $C_{25}H_{16}N_4O$: C, 77.29 (77.30); H, 4.12 (4.15); N, 14.40 (14.42); O, 4.11 (4.12).

PIPP-F. Yield: 146mg, 54%. ^1H NMR (500 MHz, CDCl$_3$, ppm):δ 13.09 (s, 1 H),9.25 (d, 1 H), 9.10 (t, 1 H), 9.01 (d, 1 H), 7.90-7.80 (m, 4 H), 7.68 (d, 2 H), 7.33 (d, 2 H), 7.11 (q, 1 H), 7.00 (t, 1 H), 6.43 (d, 1 H).^{13}C NMR (125 MHz, CDCl$_3$, ppm): δ 206.9, 149.6, 148.5, 137.9, 131.5, 130.4, 128.6, 128.1, 123.8, 122.6, 122.5, 119.1, 118.2, 112.2. HRMS Calcd for [$C_{25}H_{15}FN_4O$]: 406.41 m/z, Found: 405.94 m/z. Anal. Found (Calc) for $C_{25}H_{15}FN_4O$: C, 73.55 (73.88); H, 3.73 (3.72); N, 13.70 (13.79); O, 3.93 (3.94).

PIPP-OMe. Yield: 182 mg, 63 %. ^1H NMR (500 MHz, CDCl$_3$, ppm):δ 12.74 (s, 1 H),9.22 (s, 1 H), 9.08 (s, 1 H), 9.00 (d, 1 H), 7.84-7.78 (m, 4 H), 7.74-7.72 (m, 2 H), 7.31 (t, 2 H), 7.09 (d, 1 H), 6.88 (d, 1 H), 6.38 (d, 1 H), 3.31 (s, 3 H).^{13}C NMR (125 MHz, CDCl$_3$, ppm): δ207.0, 153.3, 151.3, 148.3, 138.6, 133.4, 131.3, 131.1, 129.0, 125.9, 123.8, 119.2, 119.0, 109.6. 55.2. HRMS Calcd for [$C_{26}H_{18}N_4O_2$]: 418.45 m/z, Found: 418.14 m/z. Anal. Found (Calc) for $C_{26}H_{18}N_4O_2$: C, 74.65 (74.63); H, 4.33 (4.34);N, 13.36 (13.39); O, 7.66 (7.65).

PIPN. Yield: 308 mg, 73 %. ^1H NMR (500 MHz, DMSO-d$_6$, ppm): δ 9.63 (s, 1 H), 9.05 (d, 1 H), 8.99 (m, 1 H), 8.92 (d, 1 H), 8.10 (d, 1 H), 7.99 (d, 1 H), 7.93 (d, 2 H), 7.83 (q, 3 H), 7.48 (d, 1 H), 7.38 (m, 5 H), 7.16 (d, 1 H). ^{13}C NMR (125 MHz, DMSO-d$_6$, ppm): δ 205.7, 147.1, 146.5,

146.4, 139.7, 130.1, 129.0, 128.1 127.0, 125.9, 125.0, 124.6, 124.1, 124.0, 122.9, 122.6, 109.7. HRMS Calcd for $[C_{29}H_{18}N_4O]$: 438.48 m/z, Found: 438.14 m/z. Anal. Found (Calc) for $C_{29}H_{18}N_4O$: C, 79.41 (79.44); H, 4.12 (4.14); N, 12.75 (12.78); O, 3.66 (3.65).

Spectroscopic measurements: The steady-state UV-visible absorption and emission spectra of the four ESIPT compounds were measured using a Shimadzu UV-2600 and FL spectrometer LS 55 (PerkinElmer), respectively. The sub-picosecond time-resolved absorption spectra were collected using a pump–probe transient absorption spectroscopy system. The pump light was generated using a regenerative amplified titanium sapphire laser system (Spectra Physics, Spitfire Ace, 1 kHz) pumped by a diode-pumped Q-switched laser (Spectra Physics, Empower). The seed pulse was generated using a titanium sapphire laser (Spectra Physics, MaiTai SP). The pulses (330 nm) generated from an optical parametric amplifier (Spectra Physics, OPAS prime) were used as the excitation beam. A white light continuum pulse, which was generated by focusing the residual of the fundamental light onto a 1 mm path length quartz cell containing water, was used as a probe beam. The white light was directed to the sample cell with an optical path of 2.0 mm and detected with a CCD detector installed in the absorption spectroscopy system after the controlled optical delay. The pump pulse was chopped by a mechanical chopper synchronized to one-half of the laser repetition rate, resulting in a pair of spectra with and without the pump, from which the absorption change induced by the pump pulse was estimated.

Density Functional Theory (DFT) and Time Dependent DFT (TDDFT) calculations: The optimized ground-state structures of PIPP-Xs (X = H, F, and OMe) and PIPN were obtained from DFT calculations using the CAM-B3LYP functional with def2-TZVP basis sets. For the geometry optimizations in the S_1 state, TDDFT calculations were implemented. Solvent effects of DCM in S_0 and S_1 were included by using the conductive polarizable continuum model (CPCM) for all the calculations. The minimum and transition states were confirmed by vibrational normal mode analysis. All calculations were performed using Gaussian 16 (version B.01) software.[1]

Reference

(1) Frisch, M. J.; Trucks, G. W.; Schlegel, H. B.; Scuseria, G. E.; Robb, M. A.; Cheeseman, J. R.; Scalmani, G.; Barone, V.; Petersson, G. A.; Nakatsuji, H.; et al. *Gaussian 16 Rev. B.01*; Wallingford, CT, 2016.

Table S1. Summary of the relative energies of singlet and triplet state E*, *cis*-K, and *per*-K* tautomers. The energy level of *cis*-K(S$_0$,vertical) and *per*-K(S$_0$,vertical), which is indicated by a dotted line, used the optimized structures of corresponding *cis*-K*(S$_1$) state. The energy unit is eV
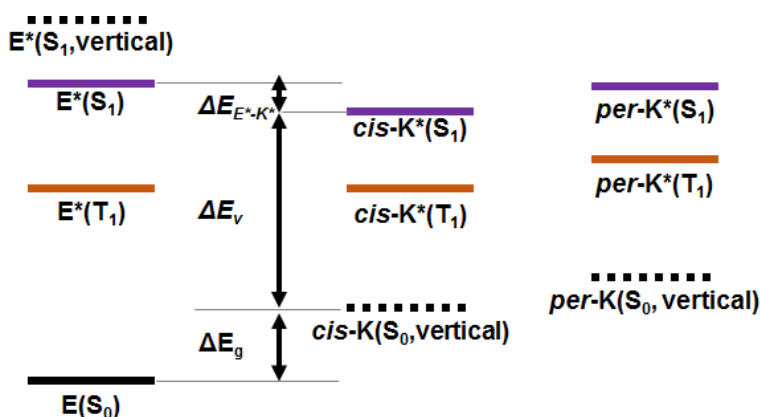
	PIPP-H	PIPP-F	PIPP-OMe	PIPN
λ_{max}(Exp.)-Absorption	3.75	3.65	3.52	3.18
λ_{max}(Exp.)-Emission	2.61	2.55	2.37	2.72
E(E(S$_1$,vertical))	3.99	4.00	3.91	4.09
E(E*(S$_1$))	3.69	3.63	3.56	3.47
E(*cis*-K*(S$_1$))	3.64	3.52	3.37	3.49
E(*per*-K*(S$_1$))	3.99	3.84	3.70	3.47
E(E*(T$_1$))	2.83	2.80	2.74	2.45
E(*cis*-K*(T$_1$))	2.89	2.68	2.47	2.77
E(*per*-K*(T$_1$))	3.24	3.17	2.94	3.11
$\Delta E_{E^*-K^*}$	0.05	0.11	0.19	-0.02
ΔE_v(vertical)	2.97	2.93	2.63	2.72
ΔE_g	0.67	0.60	0.74	0.77

Table S2. Summary of the NPA(natural population analysis) charges of important moieties and atoms in E*, *cis*-K, and *per*-K* tautomers

E*

cis-K* and *per*-K*
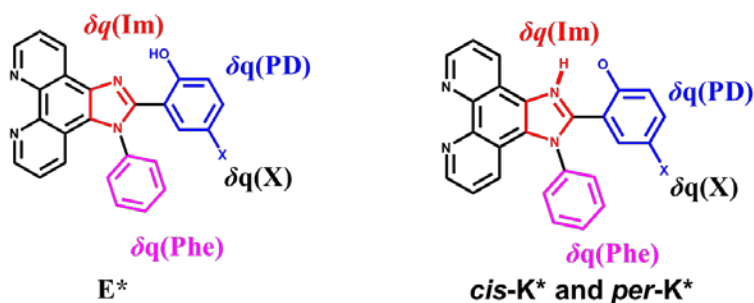
	PIPP-H			PIPP-F			PIPP-OMe			PIPN		
	E*	*cis*-K*	*per*-K*	E*	*cis*-K*	*per*-K*	E*	*cis*-K*	*per*-K*	E*	*cis*-K*	*per*-K*
δq(PD)	0.015	-0.455	-0.059	0.023	-0.499	-0.069	0.129	-0.430	-0.053	0.062	-0.472	-0.045
δq(Phenolate)[a]	-0.525	-0.455	-0.059	-0.516	-0.499	-0.069	-0.407	-0.430	-0.053	-0.478	-0.472	-0.045
δq(Phe)	0.263	0.259	0.224	0.268	0.275	0.200	0.256	0.230	0.221	0.246	0.259	0.225
δq(Im)	-0.122	0.280	-0.054	-0.137	0.298	-0.019	-0.240	0.326	-0.058	-0.226	-0.200	-0.099
δq(O)	-0.721	-0.676	-0.571	-0.700	-0.677	-0.567	-0.690	-0.517	-0.519	-0.718	-0.705	-0.591
δq(H)	0.539	0.493	0.460	0.539	0.496	0.460	0.536	0.493	0.459	0.540	0.505	0.458
δq(X)	0.258	0.255	0.264	-0.358	-0.353	-0.339	-0.165	-0.160	-0.151	-	-	-

a: δq(Phenolate) = δq(PD)-δq(H) for E* and δq(Phenolate) = δq(PD) for *cis*-K* and *per*-K*.

Figure S1. a) ^{1}H- and b) ^{13}C{^{1}H}-NMR data for PIPP-H in CDCl$_3$.
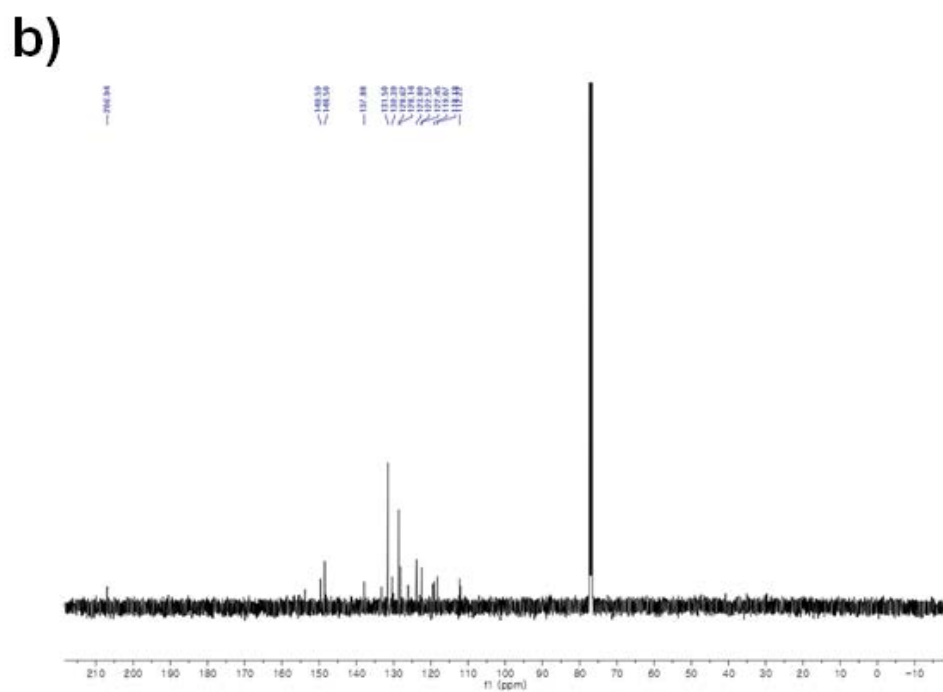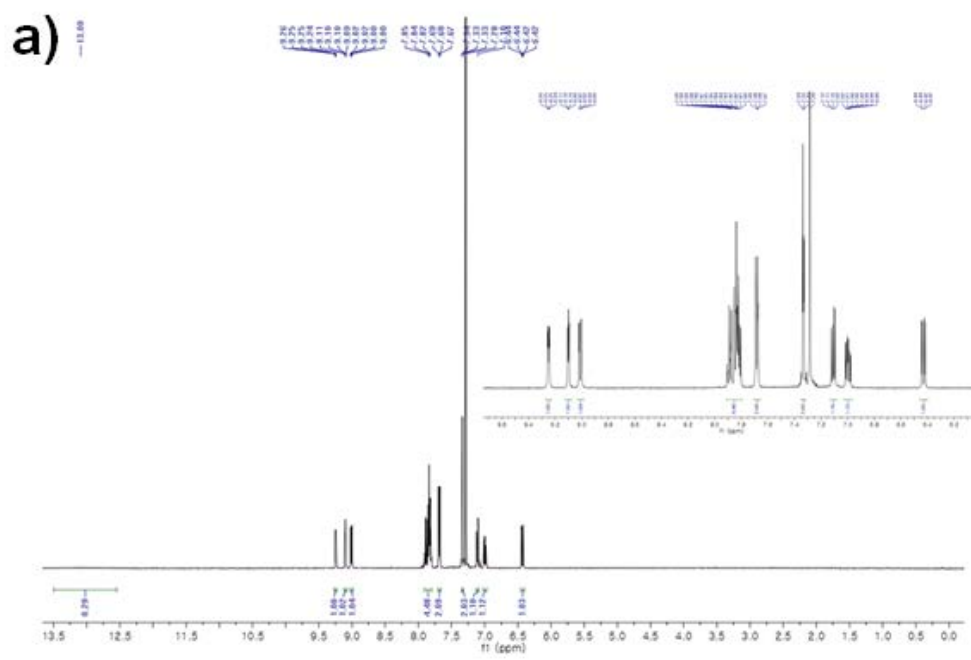
Figure S2. a) ^{1}H- and b) ^{13}C{^{1}H}-NMR data for PIPP-F in CDCl$_3$.

Figure S3. a) ^{1}H- and b) ^{13}C{^{1}H}-NMR data for PIPP-OMe in CDCl$_3$.

Figure S4. a) ^{1}H- and b) ^{13}C{^{1}H}-NMR data for PIPN in DMSO-D$_6$.

a)

PIPP-H (E)

PIPP-F (E)

PIPP-OMe (E)

PIPN (E)

○ H
● C
● N
● O
○ F

R(O-H)/r(N-H)/R(CC$_{twist}$)
=1.000/1.636/1.471 Å
θ(CCCN) = 0°

R(O-H)/r(N-H)/R(CC$_{twist}$)
=0.992/1.640/1.471 Å
θ(CCCN) = 0°

R(O-H)/R(N-H)/r(CC$_{twist}$)
=0.997/1.652/1.472 Å
θ(CCCN) = 0°

R(O-H)/r(N-H)/R(CC$_{twist}$)
=0.976/2.024/1.473 Å
θ(CCCN) = 51.3°

b)

PIPP-H (E*)

PIPP-H (TS, E*->K*)

PIPP-H (cis-K*)

PIPP-H (per-K*)

PIPP-H (trans-K*)

R(O-H)/R(N-H)/R(CC$_{twist}$)
=1.007/1.613/1.403 Å
θ(CCCN) = 0°

R(O-H)/R(N-H)/R(CC$_{twist}$)
=1.234/1.234/1.400 Å
θ(CCCN) = 0°

R(O-H)/R(N-H)/R(CC$_{twist}$)
=1.874/1.025/1.417 Å
θ(CCCN) = 17.1°

R(O-H)/R(N-H)/R(CC$_{twist}$)
=4.305/1.010/1.469 Å
θ(CCCN) = 110.3°

R(O-H)/R(N-H)/R(CC$_{twist}$)
=4.466/1.010/1.427 Å
θ(CCCN) = 141.3°

PIPP-F (E*)

PIPP-F (TS, E*->K*)

PIPP-F (cis-K*)

PIPP-F (per-K*)

PIPP-F (trans-K*)

R(O-H)/R(N-H)/R(CC$_{twist}$)
=1.012/1.599/1.400 Å
θ(CCCN) = 0°

R(O-H)/R(N-H)/R(CC$_{twist}$)
=1.212/1.255/1.401 Å
θ(CCCN) = 0°

R(O-H)/R(N-H)/R(CC$_{twist}$)
=1.767/1.027/1.416 Å
θ(CCCN) = 17.1°

R(O-H)/R(N-H)/R(CC$_{twist}$)
=3.912/1.010/1.472 Å
θ(CCCN) = 71.0°

R(O-H)/R(N-H)/R(CC$_{twist}$)
=4.488/1.010/1.427 Å
θ(CCCN) = 142.4°

PIPP-OMe (E*)

PIPP-OMe (TS, E*->K*)

PIPP-OMe (cis-K*)

PIPP-OMe (per-K*)

PIPP-OMe (trans-K*)

R(O-H)/R(N-H)/R(CC$_{twist}$)
=1.032/1.538/1.408 Å
θ(CCCN) = 0°

R(O-H)/R(N-H)/R(CC$_{twist}$)
=1.178/1.289/1.410 Å
θ(CCCN) = 0°

R(O-H)/R(N-H)/R(CC$_{twist}$)
=1.796/1.026/1.420 Å
θ(CCCN) = 13.7°

R(O-H)/R(N-H)/R(CC$_{twist}$)
=3.628/1.011/1.470 Å
θ(CCCN) = 107.0°

R(O-H)/R(N-H)/R(CC$_{twist}$)
=4.467/1.009/1.430 Å
θ(CCCN) = 140.5°

PIPN (E*)

PIPN (TS, E*->K*)

PIPN (cis-K*)

PIPN (per-K*)

R(O-H)/R(N-H)/R(CC$_{twist}$)
=1.004/1.646/1.404 Å
θ(CCCN) = 25.4°

R(O-H)/R(N-H)/R(CC$_{twist}$)
=1.264/1.210/1.408 Å
θ(CCCN) = 21.6°

R(O-H)/R(N-H)/R(CC$_{twist}$)
=1.983/1.022/1.428 Å
θ(CCCN) = 39.7°

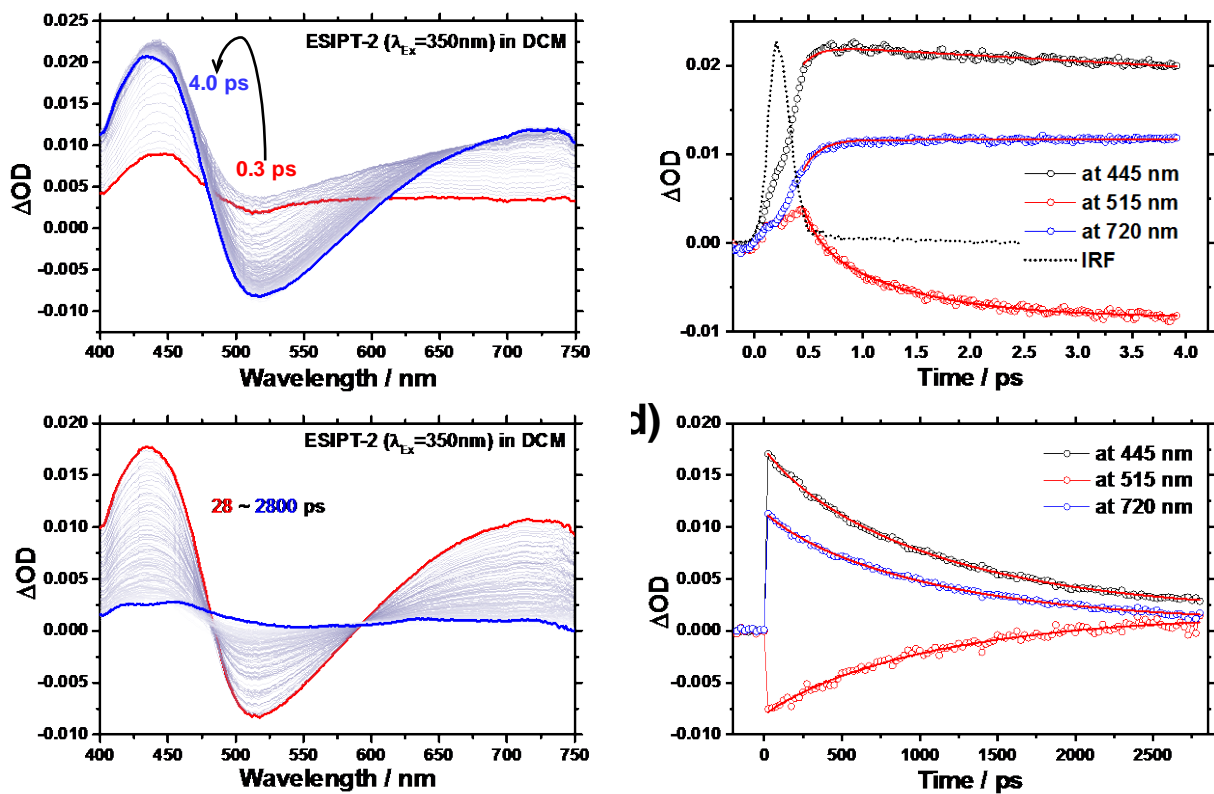R(O-H)/R(N-H)/R(CC$_{twist}$)
=3.577/1.012/1.461 Å
θ(CCCN) = 106.6°

Figure S5. DFT and TDDFT optimized structures of four ESIPT compounds in the a) ground (S_0) state and b) S_1 state.

Figure S6. a and c) Transient absorption spectra of PIPP-F in DCM with the excitation wavelength of 350 nm. b and d) Decay profiles monitored at selected wavelengths (black circle: 445 nm, red circle: 515 nm, and blue circle: 720 nm). The instrument response function (IRF) is shown as black dotted line. Theoretical fitting curves are shown as red solid line.
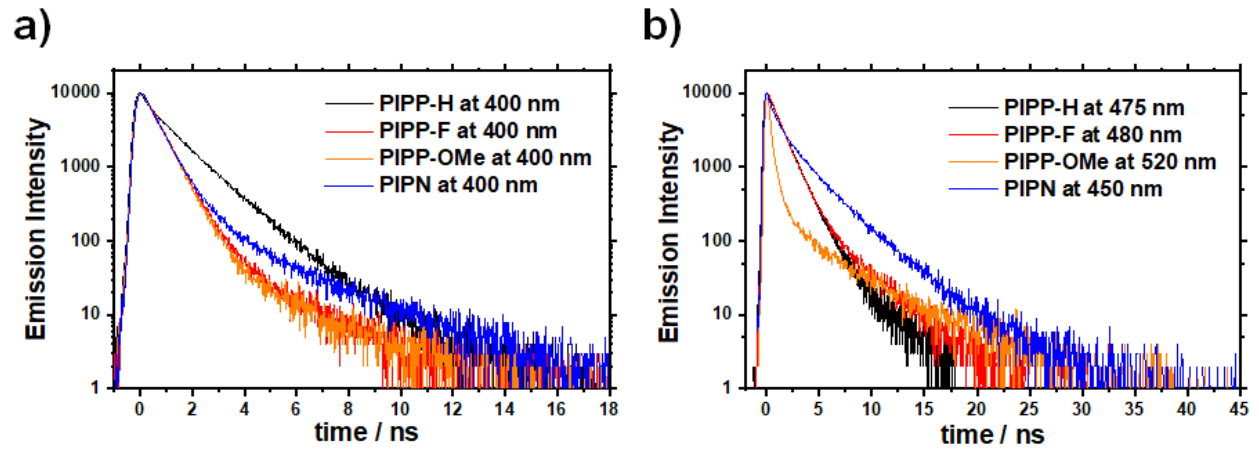
Figure S7. Fluorescence decay profiles for four ESIPT compounds in DCM. Excitation wavelength is 375 nm.
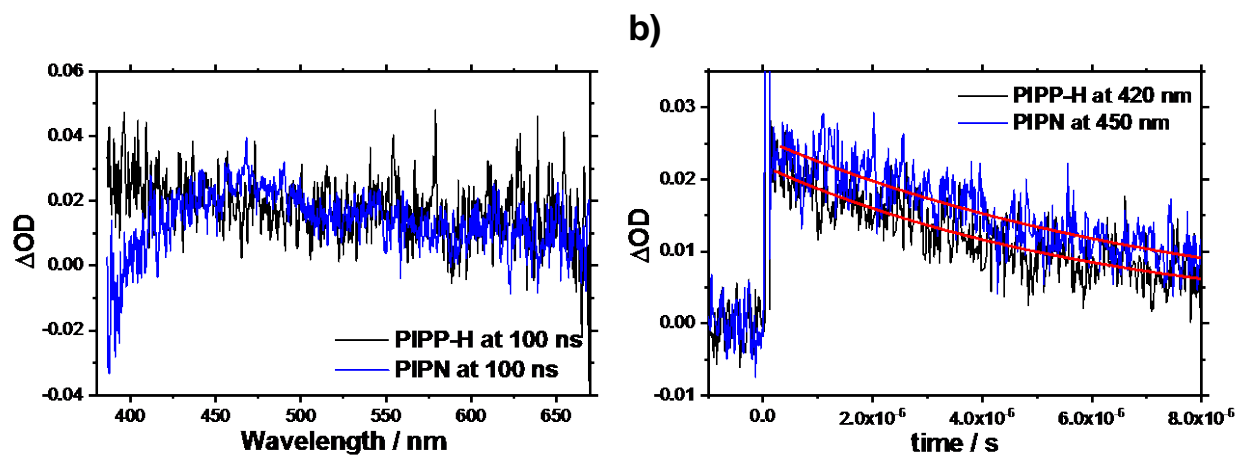
Figure S8. a) Nanosecond Transient absorption spectra of PIPP-H and PIPN in DCM. b) Decay profiles of PIPP-H and PIPN recorded at 420 and 450 nm, respectively.
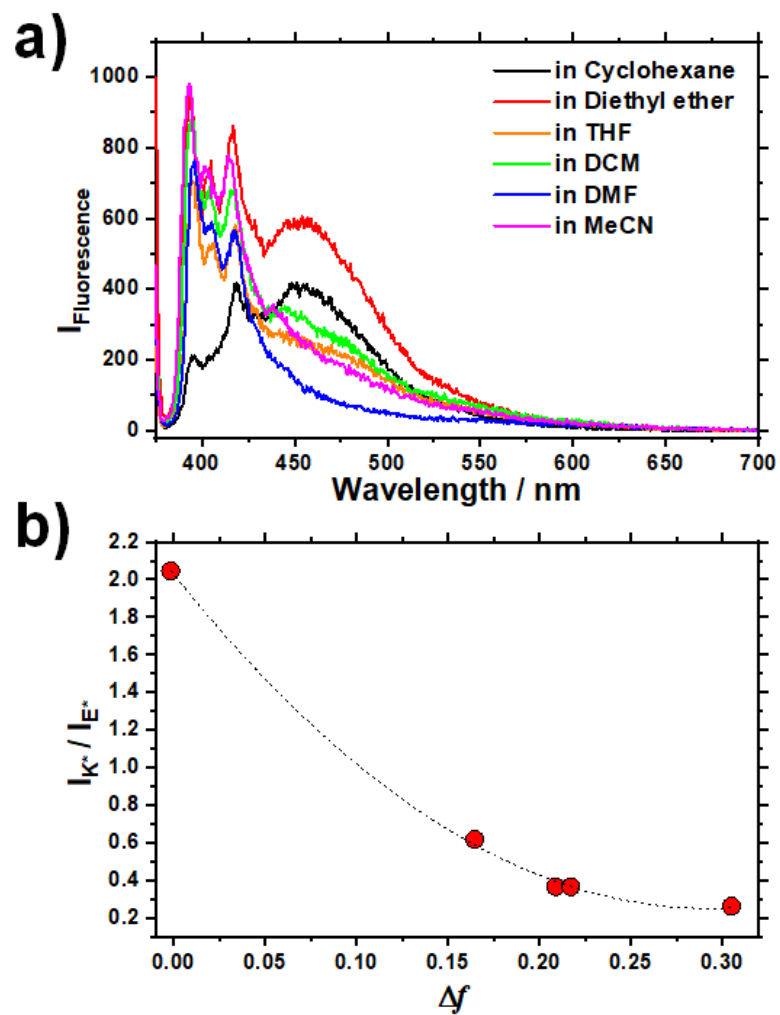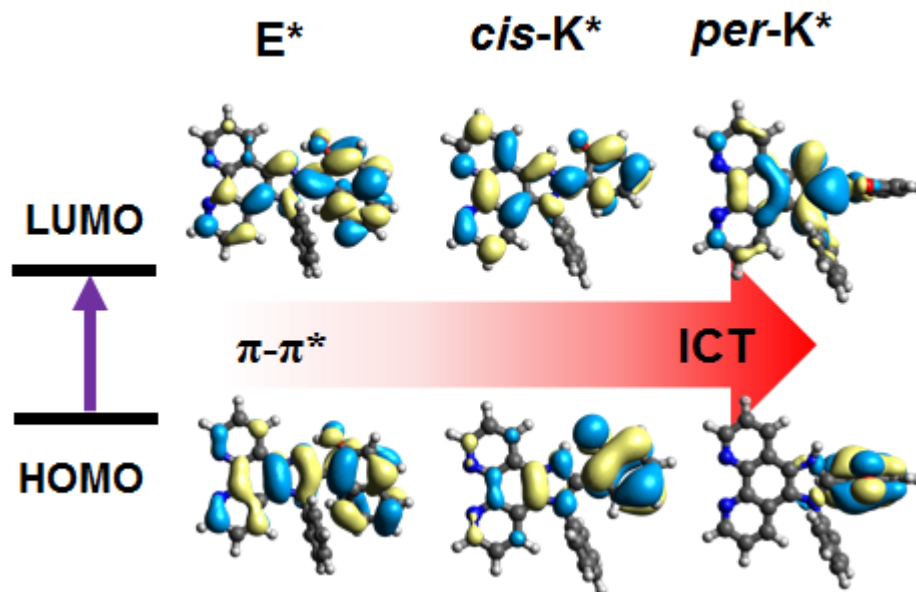
Figure S9. (a) Emission spectra of PIPN measured in various solvents with the excitation wavelength of 370 nm. b) The intensity ratio of the E* and K* band, I_{K*}/I_{E*}, for PIPN against the orientation polarizability (Δf).
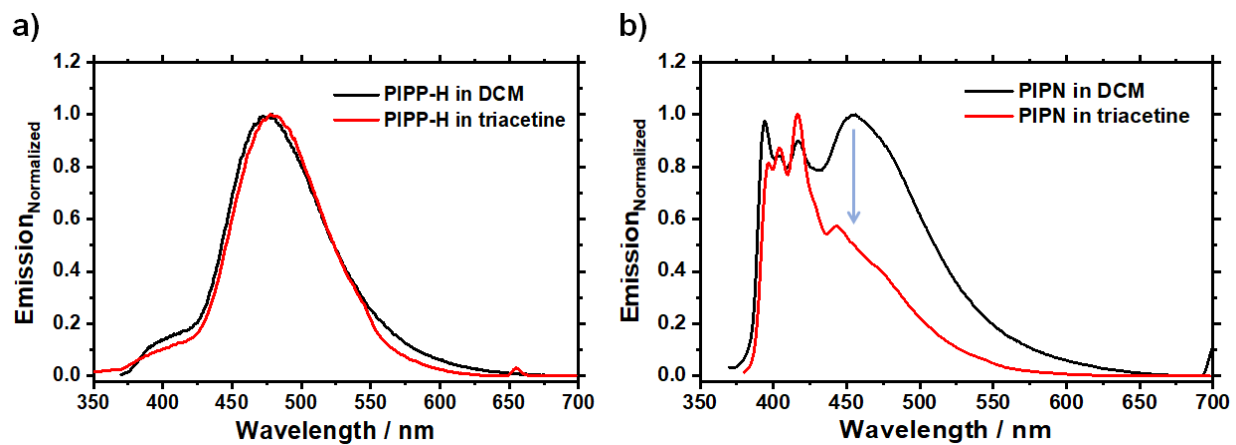
Figure S10. Emission spectra of PIPP-H and PIPN in DCM and triacetin. The viscosities of DCM and triacetin at 20 °C are 0.43 and 23 cP, respectively.

Figure S11. TDDFT calculated HOMO and LUMO orbitals for each tautomer in PIPN. HOMO-LUMO transition contributes to the lowest electronic transition (S_1) of PIPN dominantly. The π-π* transitions to form the E* and *cis*-K* tautomers are changed to the charge transfer transition in *per*-K* geometry.
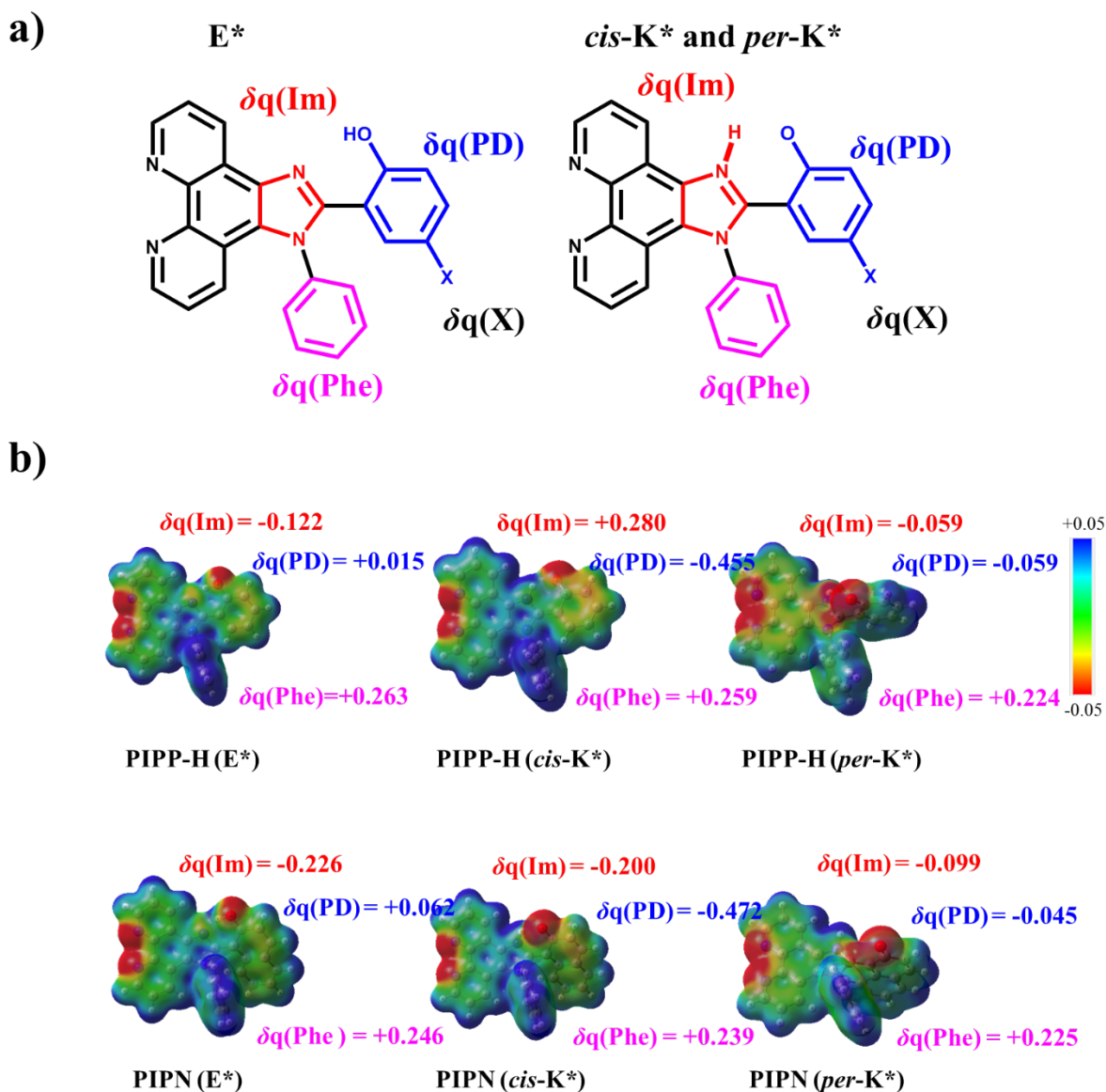
Figure S12. Electrostatic potential maps and partial charges of each moiety for E*, *cis*-K*, and *per*-K* tautomers of PIPP-H and PIPN. a) Definitions of partial charges in enol- and keto-tautomers in S_1 state, and b) Electrostatic potential maps and specific values of partial charges.